Title

Neuroglian regulates Drosophila intestinal stem cell proliferation through enhanced signaling via the epidermal growth factor receptor

Journal

Stem Cell Reports, 16(6)

ISSN

2213-6711

Authors

Resnik-Docampo, Martin
Cunningham, Kathleen M
Ruvalcaba, S Mateo
et al.

Publication Date

2021-06-01

DOI

10.1016/j.stemcr.2021.04.006

Peer reviewed

Stem Cell Reports
Article

ISSCR

OPEN ACCESS

Neuroglian regulates *Drosophila* intestinal stem cell proliferation through enhanced signaling via the epidermal growth factor receptor

Martin Resnik-Docampo,[1,4] Kathleen M. Cunningham,[1,4] S. Mateo Ruvalcaba,[1] Charles Choi,[1] Vivien Sauer,[1] and D. Leanne Jones[1,2,3,5,*]

[1]Department of Molecular, Cell and Developmental Biology, University of California, Los Angeles, Los Angeles, CA 90095, USA
[2]Molecular Biology Institute, University of California, Los Angeles, Los Angeles, CA 90095, USA
[3]Eli and Edythe Broad Center of Regenerative Medicine and Stem Cell Research, University of California, Los Angeles, Los Angeles, CA 90095, USA
[4]These authors contributed equally
[5]Present address: Departments of Anatomy and Medicine, Division of Geriatrics, Eli and Edythe Broad Center for Regeneration Medicine, University of California, San Francisco, San Francisco, CA 94143, USA
*Correspondence: leanne.jones@ucsf.edu
https://doi.org/10.1016/j.stemcr.2021.04.006

SUMMARY

The *Drosophila* intestine is an excellent system for elucidating mechanisms regulating stem cell behavior. Here we show that the septate junction (SJ) protein Neuroglian (Nrg) is expressed in intestinal stem cells (ISCs) and enteroblasts (EBs) within the fly intestine. SJs are not present between ISCs and EBs, suggesting Nrg plays a different role in this tissue. We reveal that Nrg is required for ISC proliferation in young flies, and depletion of Nrg from ISCs and EBs suppresses increased ISC proliferation in aged flies. Conversely, overexpression of Nrg in ISC and EBs promotes ISC proliferation, leading to an increase in cells expressing ISC/EB markers; in addition, we observe an increase in epidermal growth factor receptor (Egfr) activation. Genetic epistasis experiments reveal that *Nrg* acts upstream of *Egfr* to regulate ISC proliferation. As Nrg function is highly conserved in mammalian systems, our work characterizing the role of Nrg in the intestine has implications for the treatment of intestinal disorders that arise due to altered ISC behavior.

INTRODUCTION

Adult stem cells maintain tissue homeostasis through the balanced generation of new daughter stem cells and progenitor cells destined to differentiate. In addition, adult stem cells serve as a reservoir of cells for the repair of tissues and organs after damage. Studies have shown that age-related changes in stem cell function likely lead to a loss of homeostasis over time and may contribute to age-onset disease (Jones and Rando, 2011). Therefore, understanding the mechanisms involved in regulating stem cell behavior and how these mechanisms are altered with age will uncover therapeutic targets for regenerative medicine in order to treat age-onset and/or degenerative diseases.

The *Drosophila* midgut, the functional equivalent to the mammalian small intestine, is maintained over time by resident intestinal stem cells (ISCs) (Micchelli and Perrimon, 2006; Ohlstein and Spradling, 2006). The ISCs are multipotent and divide to produce more ISCs or enteroblasts (EBs) that differentiate into absorptive enterocytes (ECs) or secretory enteroendocrine cells (EEs), all of which are needed to maintain homeostasis. Additional reports suggest that ISCs can differentiate into EEs directly, without progressing through the EB state (Amcheslavsky et al., 2014; Biteau and Jasper, 2014; Guo and Ohlstein, 2015; Zeng and Hou, 2015). Several highly conserved signaling pathways, for example, the epidermal growth factor receptor (EGFR) and Notch pathways, play essential roles in regulating ISC proliferation and differentiation, respectively (Li and Jasper, 2016; Nászai et al., 2015). EGFR/MAPK signaling acts as a permissive signal for proliferation in ISCs, coordinating with JAK/STAT signaling to regulate ISC growth and division (Biteau and Jasper, 2011; Buchon et al., 2010; Cordero et al., 2012; Jiang et al, 2009, 2011; Jin et al., 2015; Xu et al., 2011). EGF ligands and the Egfr itself are responsive to additional, conserved homeostatic or stress signals integrated from the environment (Buchon et al., 2010; Cordero et al., 2012; Du et al., 2020; Ngo et al., 2020; Zhang et al., 2019). Remarkably, similar observations have been made in the mammalian intestine, emphasizing the usefulness of the fly intestine as a model to uncover conserved mechanisms regulating ISC behavior (Jasper, 2020).

A number of age-related changes occur in the fly intestine, such as increased ISC proliferation, accumulation of EB-like cells that express ISC markers as well as hallmarks of differentiated cells, bacterial dysbiosis, and loss of the intestinal barrier (Jasper, 2020). In flies and mammals, disruption of intestinal barrier function and increased intestinal permeability correlate with compromised integrity of the cell-cell junctions, known as occluding junctions (Marchiando et al., 2010; Rera et al., 2012; Resnik-Docampo et al., 2017; Vancamelbeke and Vermeire, 2017). These specialized structures—tight junctions in vertebrates and septate junctions (SJs) in arthropods—regulate paracellular flow between apical and basal epithelial surfaces. In a previous study investigating age-related changes to the intestinal barrier, we found that the SJ protein Neuroglian (Nrg) is

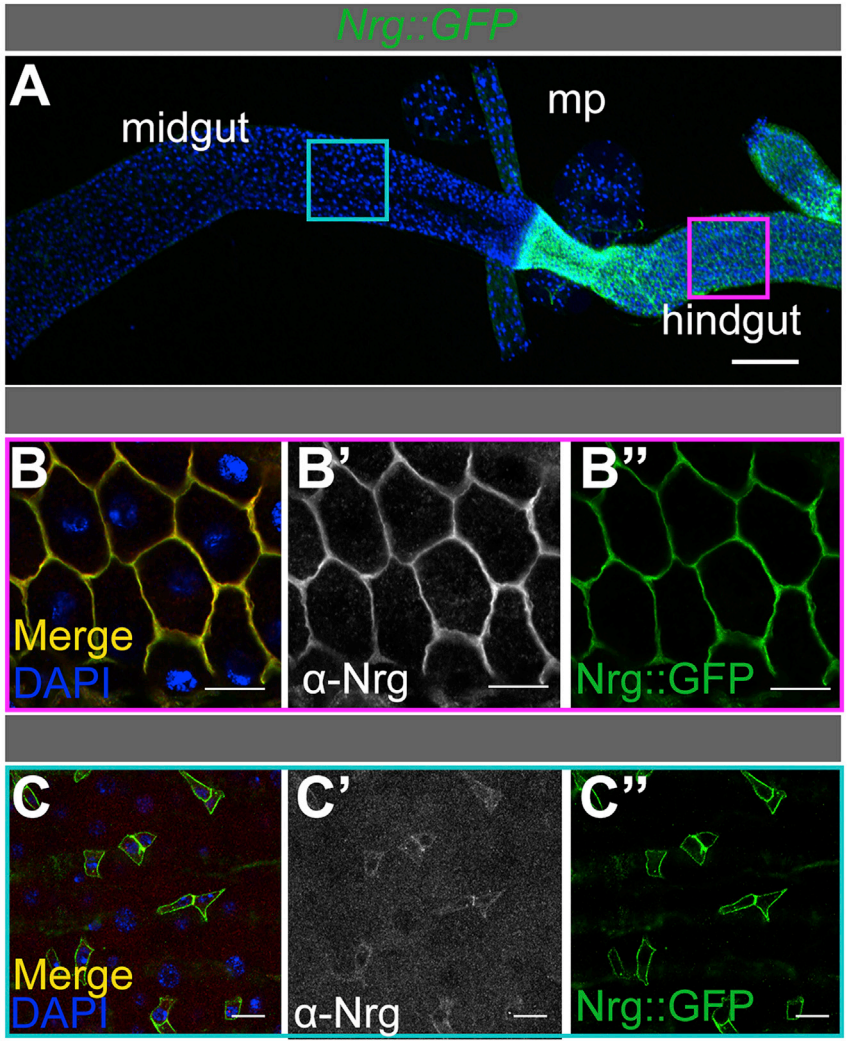

Figure 1. Neuroglian (Nrg) is expressed in the ISCs and EBs of the *Drosophila* midgut

(A) Representative low-magnification image of Nrg::GFP (green) expression in the adult gut, including the midgut, Malpighian tubules (mp), and hindgut. Scale bar, 100 μm. (B and C) Adult hindgut (B, magenta border) and midgut (C, teal border) of an adult expressing Nrg::GFP (B, B″, C, and C″) and stained with anti-Nrg antibody (B, B′, C, and C′) (see experimental procedures). Note expression of Nrg in ISC and EB nests of the midgut. Scale bars, 20 μm. See also Figure S1.

strongly expressed in the hindgut (Resnik-Docampo et al., 2017). However, we also observed expression within ISC and EB "nests" in the midgut. Here, we describe a role for Nrg in regulating ISC behavior through potentiation of signaling via the Egfr in both young and aged flies.

RESULTS

Nrg is expressed in ISC and EB nests in the *Drosophila* posterior midgut

Our lab previously reported the expression of known SJ proteins in the fly intestine and described how expression and localization patterns change as a consequence of aging (Resnik-Docampo et al., 2017). While the SJ protein Nrg was strongly expressed in the pleated SJs in the *Drosophila* hindgut (Figures 1A and 1B–B″), Nrg was also detected in ISC and EB nests that express the canonical marker Escargot (Esg) (Figures 1A, 1C–C″, and S1A–S1A′). By contrast, no Nrg was detected in ECs within the midgut, consistent with previous observations (Baumann, 2001).

Two different protein isoforms of Nrg differ at the C-terminal cytoplasmic domain: a neuronal-specific isoform, Nrg^{180}, and another generally expressed isoform, Nrg^{167} (Hortsch et al., 1990). To confirm that an Nrg::GFP fusion protein accurately reflects Nrg protein expression, we generated an antibody that detects both Nrg isoforms (see experimental procedures); anti-Nrg antibody specificity was confirmed using depletion of Nrg via RNAi in wing imaginal discs (Figures S1B–S1C′). Using the antibody, confocal immunofluorescence (IF) microscopy confirmed endogenous Nrg expression and localization patterns in the hindgut and midgut (Figures 1A, 1B, 1B′, 1C, and 1C′). Consistent with our observations, recent single-cell sequencing data profiling of the *Drosophila* midgut found

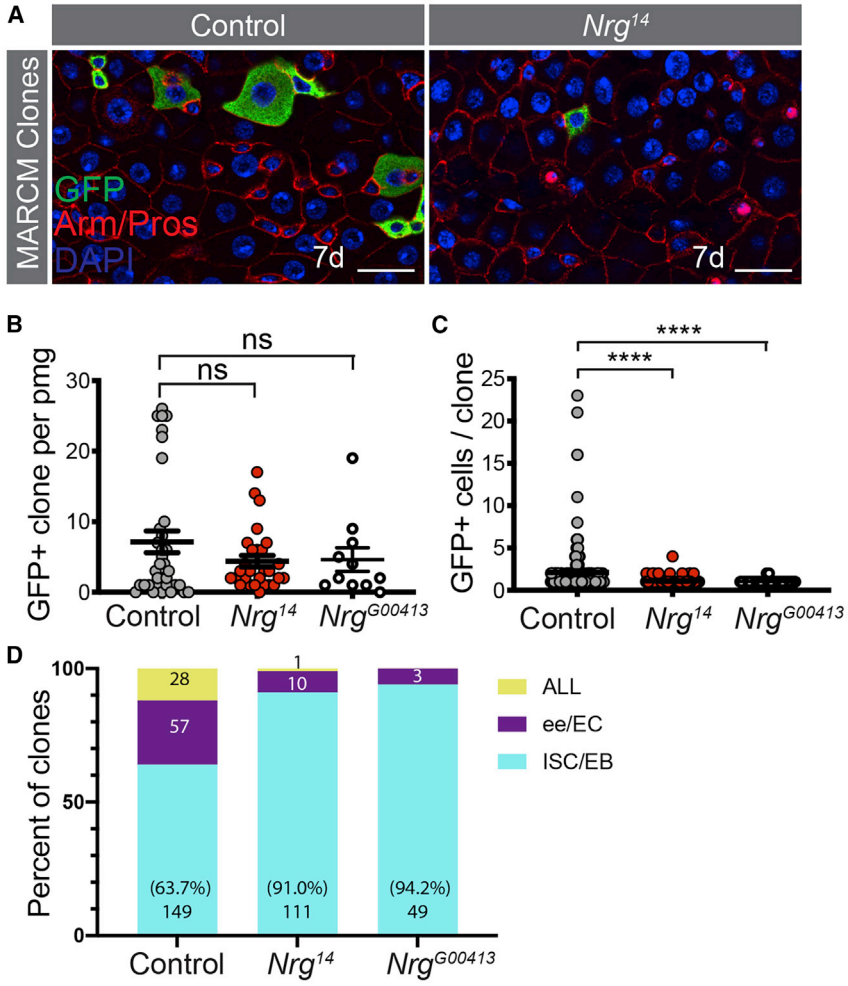

Figure 2. Nrg is required for ISC proliferation

(A) Examples of midguts 7 days after FRT-mediated clonal generation in control and Nrg^{14} backgrounds. Clones are positively marked in green (see experimental procedures). Scale bars, 20 μm.

(B) Total number of GFP$^+$ cells (MARCM clones) per posterior midgut (pmg) in control, Nrg^{14}, and Nrg^{G00413} backgrounds. n = 34 control, 28 Nrg^{14}, and 11 Nrg^{G0041} guts; Kruskal-Wallis test followed by Dunn's multiple comparisons. ns = not significant.

(C) Quantification of number of GFP$^+$ cells per clone in 7 days after FRT-mediated clonal generation in control, Nrg^{14}, and Nrg^{G00413} backgrounds. n = 225 control, 122 Nrg^{14}, and 52 Nrg^{G0041} clones; Kruskal-Wallis test followed by Dunn's multiple comparisons. ****p < 0.0001.

(D) Characterization of the types of GFP$^+$ cells (ISCs/EBs, EEs/ECs, or all types) in (A). n = 225 control, 122 Nrg^{14}, and 52 Nrg^{G0041} clones.

All data are represented as the mean ± SEM. See also Figure S2.

Nrg among the most enriched genes in ISC/EB clusters (Hung et al., 2020). In addition, RNA-sequencing analysis performed from 5-day-old flies (Resnik-Docampo et al., 2017) revealed that the Nrg^{167} isoform is the primary isoform expressed in the intestine (Figure S1D).

As SJs are restricted to EC-EC and EC-EE junctions in the midgut (Resnik-Docampo et al., 2017), these data suggested that Nrg is likely not acting as an SJ protein in ISC and EBs. In addition to its role at the SJ, Nrg is one example of the cell adhesion molecules (CAMs) that play a role in the developing nervous system (Enneking et al., 2013; Goossens et al., 2011; Kristiansen et al., 2005; Kudumala et al., 2013; Moscoso and Sanes, 1995). In this context, Nrg has been demonstrated to modulate EGFR/fibroblast growth factor receptor (FGFR) signaling in order to regulate axon extension and guidance in sensory neurons (García-Alonso et al., 2000; Islam et al., 2003; Nagaraj et al., 2009). In mammals, the role of the Nrg homolog L1CAM is conserved in nervous system development (Dahme et al., 1997; Godenschwege et al., 2006; Jouet et al., 1994; Kudumala et al., 2013; Schäfer and Altevogt, 2010), and L1CAM interactions with EGFR/FGFR are also preserved in mammalian cells (Donier et al., 2012; Islam et al., 2004; Kulahin et al., 2008). Interestingly, human *L1CAM* (*hL1CAM*) expression rescues *Nrg* loss-of-function phenotypes in *Drosophila*, demonstrating a remarkable conservation of function (Godenschwege et al., 2006; Kristiansen et al., 2005; Kudumala et al., 2013).

Nrg is required for ISC proliferation in the posterior midgut

To investigate the role of Nrg in the intestine, flippase recognition target (FRT)-mediated recombination was used to generate positively marked (GFP$^+$) ISC "clones" that were homozygous mutants for either a null allele of *Nrg*, Nrg^{14} (Enneking et al., 2013), or a strong hypomorphic allele, Nrg^{G00413} (Figures 2A–2C). Wild-type, GFP$^+$ control clones were generated in parallel. Quantification of the

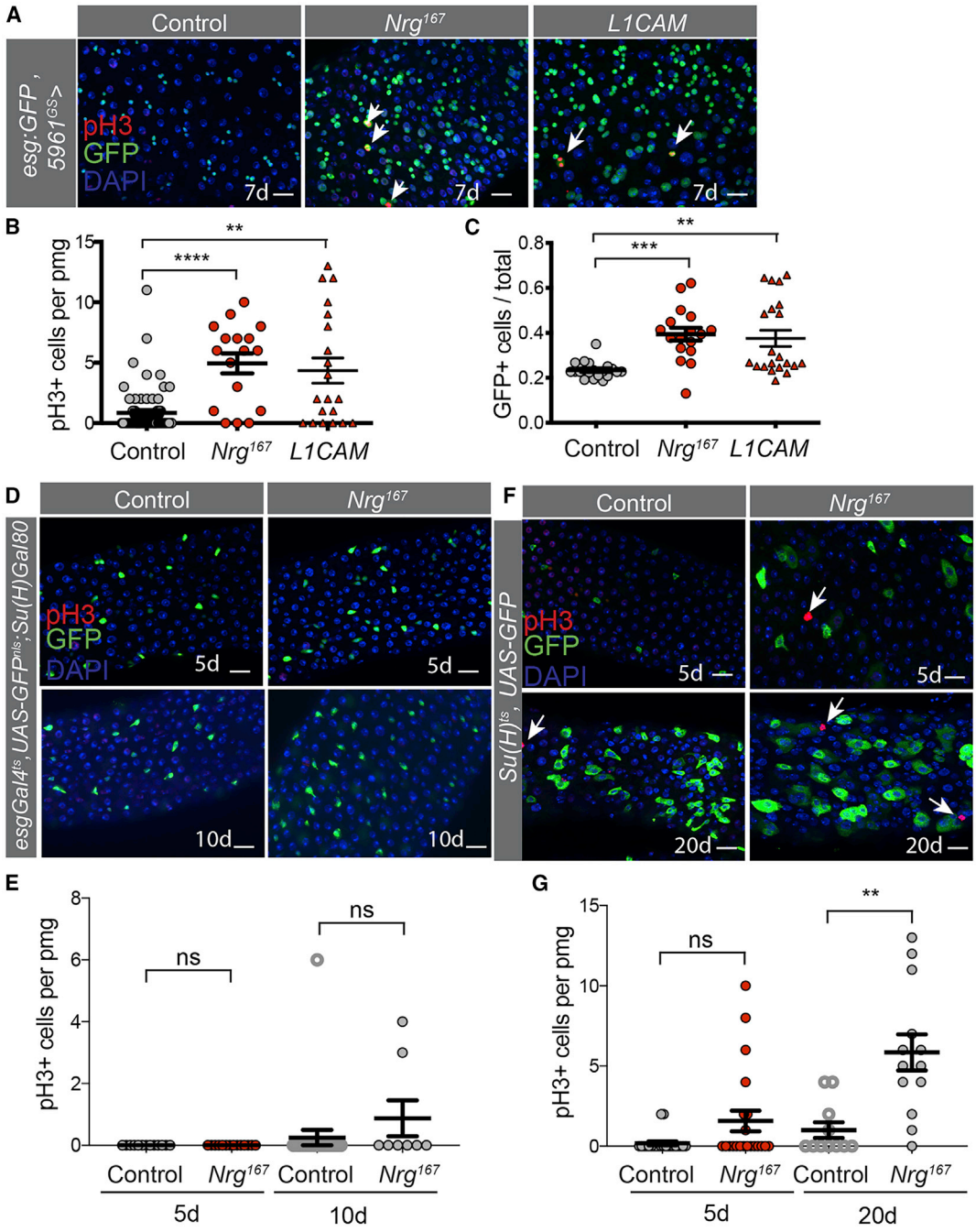

Figure 3. Overexpression of Nrg in ISCs and EBs induces ISC proliferation

(A) Representative images from adult midguts of *5961^{GS}* crossed to control (*OreR*), *UAS-Nrg^{167}*, or *UAS-hL1CAM* for 7 days. ISCs/EBs (*esg:GFP*, green), mitotic cells (pH3, red), and nuclei (DAPI, blue) are shown. Scale bars, 20 μm. White arrows indicate pH3+ cells.

(B) Quantification of number of pH3^{+} mitotic cells per pmg in (A). n = 20 control, 17 *Nrg^{167}*, and 21 *hL1CAM* guts; Kruskal-Wallis test with Dunn's multiple comparisons. **p < 0.01, ****p < 0.0001.

(C) Quantification of the number of *esg*:GFP^{+} cells per pmg in (A). Ordinary one-way ANOVA with Tukey's multiple comparisons. **p < 0.01, ***p < 0.001.

(D) Representative images from adult midguts of control (*OreR*) and *UAS-Nrg^{167}* driven in ISCs only (*esgGal4, UAS-2xYFP; Su(H)Gal80, tubGal80^{ts}*) for 5 or 10 days. ISCs (GFP, green), mitotic cells (pH3, red), and nuclei (DAPI, blue) are shown. Scale bars, 20 μm.

(legend continued on next page)

number of clones per gut 7 days post clone induction revealed no difference in frequency when comparing wild-type with Nrg^{14} or Nrg^{G00413} mutant clones, suggesting that *Nrg* mutant ISCs are not lost (Figure 2B). However, detailed analysis of the clonal cell population showed that Nrg^{14} or Nrg^{G00413} clones often consisted of single ISCs or EBs (91.0% and 94.2%, respectively), compared with controls (63.7%) (Figures 2A, 2C, and 2D). The increase in single-cell clones corresponded to a reduction in clones containing differentiated cells, with 8.2% of Nrg^{14} clones containing only EEs or ECs, compared with 24.4% for controls. Furthermore, the number of clones containing all the cell types dropped from 10.3% in controls to 0.8% in Nrg^{14} mutants and 0% in Nrg^{G00413} mutants (Figure 2D). Generation of ISC/EB clones expressing an RNAi targeting *Nrg* resulted in a similar shift to clones containing single cells (Figures S2B, S2B′, and S2E–S2G) after 14 days, compared with controls (Figure S2A, S2A′, and S2E–S2G). However, there was no decrease in the number of GFP^+ clones after 7 or 14 days (Figures S2C and S2E). Taken together, these data suggest that Nrg plays a role in regulating ISC proliferation and/or differentiation into EBs.

Nrg overexpression in ISCs and EBs induces ISC proliferation

As Nrg appeared to be required for ISC proliferation (Figures 2 and S2), we wanted to determine whether targeted overexpression of *Nrg* in ISCs and EBs was sufficient to induce proliferation. To do so, a construct encoding Nrg^{167} was overexpressed utilizing an RU486-inducible Gene-Switch "driver" line that is expressed in ISCs and EBs, 5961^{GS} (see experimental procedures). Addition of RU486 to food (RU+) leads to induction of transgene expression, while lack of RU486 (RU−) and outcrossed controls lacking the transgene serve as negative controls. Mitotic cells were detected and quantified by staining for phosphorylated histone H3 (pH3); as ISCs are the only dividing cells in the intestine, quantification of proliferation serves as a surrogate marker for the presence and activity of ISCs. After 7 days of exposure to RU486, a statistically significant increase in the number of mitotic cells was observed upon Nrg^{167} expression, compared with controls (Figures 3A and 3B). Accordingly, we observed an increase in the number of cells expressing the ISC/EB marker *esg* (Figures 3A and 3C). In previous studies in the fly nervous system, the human homolog of Nrg, hL1CAM, was found to rescue neurodevelopmental defects in *Nrg* mutants (Godenschwege et al., 2006; Kakad et al., 2018; Kudumala et al., 2013). Therefore, we tested whether human *hL1CAM* expression was also sufficient to induce ISC proliferation. Indeed, ectopic expression of *hL1CAM* in ISC and EBs with the 5961^{GS} driver also showed a significant increase in ISC proliferation, similar to Nrg^{167} (Figures 3A–3C).

Next, we wanted to distinguish whether Nrg expression in ISCs *or* EBs was sufficient to drive ISC proliferation. ISC-specific overexpression of Nrg for up to 10 days did not lead to an increase in ISC proliferation (Figures 3D and 3E), as measured by pH3 staining. By contrast, Nrg overexpression in EBs only, using the *Su(H)Gal4, UAS-GFP; tubGal80^{ts}* (referred to as $Su(H)^{ts}$) induced ISC proliferation (Figures 3F and 3G). In addition, we observed an increase in EB-like, *Su(H)Gal4>GFP*$^+$ cells, similar to what is observed when Nrg is overexpressed in ISCs and EBs simultaneously (Figure 3F). To determine whether the increase in proliferation was due to division of EB-like cells, we counted the total number of *Su(H)>GFP*$^+$, $pH3^+$ cells in guts upon Nrg overexpression. After 5 days of expression, 0/33 $pH3^+$ cells were also GFP^+, while at 20 days, 2/67 were $GFP^+/pH3^+$ double positive, indicating that the vast majority of dividing cells are ISCs.

As an independent assessment of the $pH3^+$ cells produced upon expression of Nrg, we quantified the intensity of anti-pH3 anti-β-galactosidase (β-gal) staining in GFP^+ nuclei in guts from flies expressing Nrg^{167} in ISCs and EBs (genotype: *Su(H)LacZ; 5961^{GS}>Nrg^{167}*) (Figure S3). In all of the controls (Figures S3A–S3A‴ and S3D) and the large majority of guts in which Nrg^{167} was expressed (Figures S3B–S3C‴ and S3D), $pH3^+$ cells did not express β-gal above background (33/36 $pH3^+$ cells). Taken together, these data indicate that Nrg expression in EBs can act in a non-autonomous manner to promote ISC proliferation.

Misexpression of Nrg contributes to age-related changes in the intestine

Aging results in an increase in ISC proliferation and an accumulation of EB-like cells that express hallmarks of both ISC/EBs and differentiating ECs (Biteau et al., 2008; Jiang et al., 2009; Li and Jasper, 2016; Park et al., 2009). Due to the increases in ISC proliferation and *esg*-expressing cells resulting from Nrg overexpression, we hypothesized

(E) Quantification of number of $pH3^+$ mitotic cells per pmg in (C). n = 13 control 5-do, 14 Nrg^{167} 5-do, 24 control 10-do, and 8 Nrg^{167} 5-do guts; Kruskal-Wallis test with Dunn's multiple comparisons. ns = not significant.
(F) Representative images from adult midguts of control (*OreR*) and *UAS-Nrg^{167}* driven in EBs only ($Su(H)^{ts}$) for 5 or 20 days. EBs (GFP, green), mitotic cells (pH3, red), and nuclei (DAPI, blue) are shown. Scale bars, 20 μm.
(G) Quantification of number of $pH3^+$ mitotic cells per pmg in (E). n = 22 control 5-do, 21 Nrg^{167} 5-do, 11 control 20-do, and 13 Nrg^{167} 20-do; Kruskal-Wallis test with Dunn's multiple comparisons. ns = not significant, **p < 0.01.
All data are represented as the mean ± SEM. See also Figure S3.

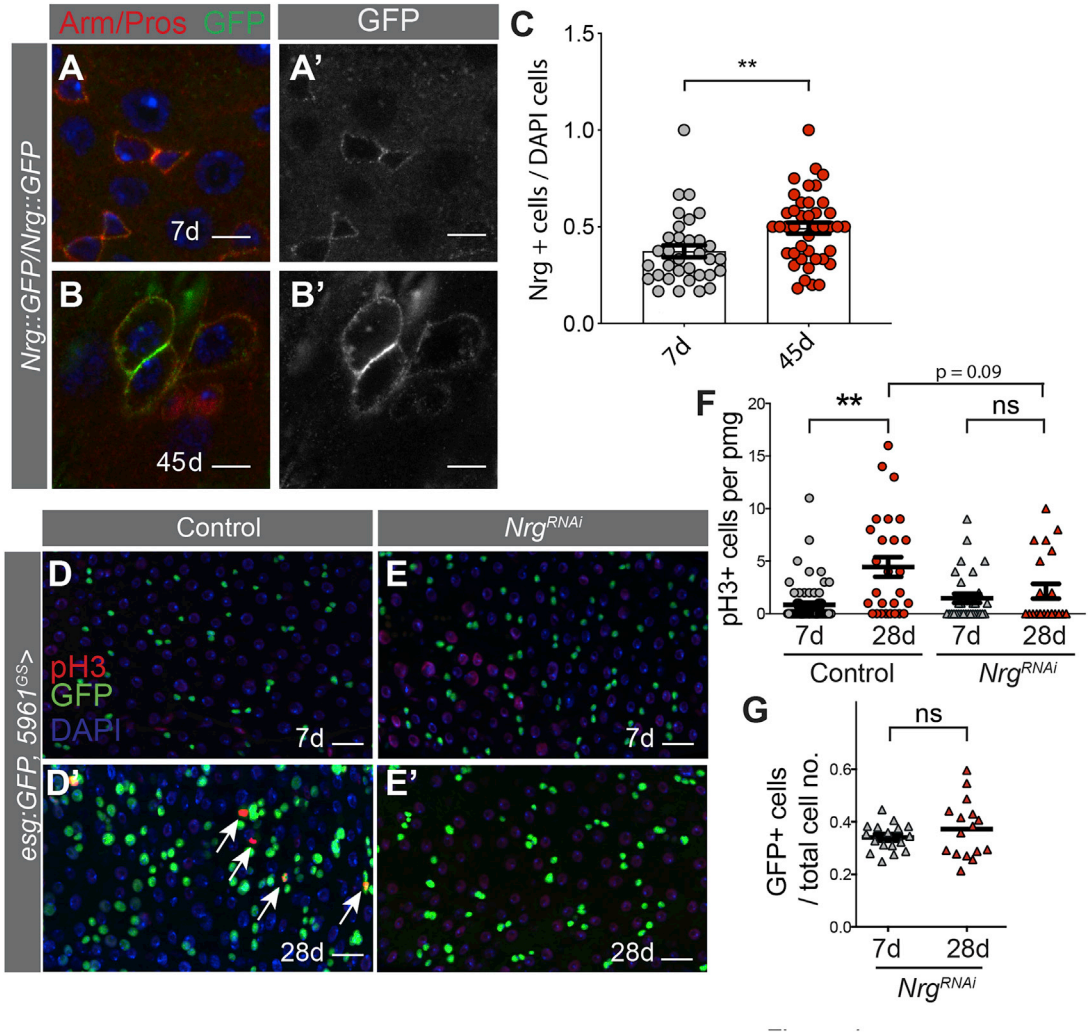

Figure 4. Misexpression of Nrg contributes to age-related changes in the intestine

(A and B) Representative images of Nrg::GFP in young (7 d, A, A′) and old (45 d, B, B′) midguts. Scale bars, 5 μm.

(C) Quantification of the number of Nrg^+ cells per total cell number in (A). n = 33 young, 41 aged per field of view (fov), unpaired two-tailed t test. **p < 0.01.

(D and E) Representative images from adult midguts from 5961^{GS} flies crossed to control (*OreR*, D, D′) or *UAS-*$Nrg^{RNAi\ V20}$ (E, E′) for 7 days (young) or 28 days (old). ISC/EBs (*esg:GFP*, green), mitotic cells (pH3, red), and nuclei (DAPI, blue) are shown. White arrows indicate pH3+ cells.

(F) Quantification of number of $pH3^+$ mitotic cells in (A) per pmg. n = 71 control 7-do, 27 control 28-do, 30 Nrg^{RNAi} 7-do, and 22 Nrg^{RNAi} 7-do guts; Kruskal-Wallis test with Dunn's multiple comparisons. ns = not significant, **p < 0.01.

(G) Quantification of the total number of ISCs/EBs (*esg:GFP*, green) in 5961^{GS}>Nrg^{RNAi} animals shown in (E and E′). n = 30 Nrg^{RNAi} 7-do and 22 Nrg^{RNAi} 28-do guts, unpaired t test.

All data are represented as the mean ± SEM. ns = not significant.

that Nrg accumulation contributes to age-related changes in the midgut. Analysis of RNA-sequencing data of old versus young fly midguts (Resnik-Docampo et al., 2017) revealed that *Nrg* expression was 1.834 ± 0.05-fold ($p = 1.61 \times 10^{-27}$) higher in midguts dissected from 45-day-old (do) flies than in the midguts of young flies. Consistent with the observed localization in ISC/EB nests and an expansion of EB-like cells with age, the number of cells expressing Nrg was also increased in intestines from aged flies (Figures 4B, 4B′, and 4C), compared with young controls (Figures 4A, 4A′, and 4C).

Based on the observation that Nrg is required for ISC proliferation in young flies (Figures 2 and S2), we hypothesized that reducing Nrg expression in ISCs and EBs would

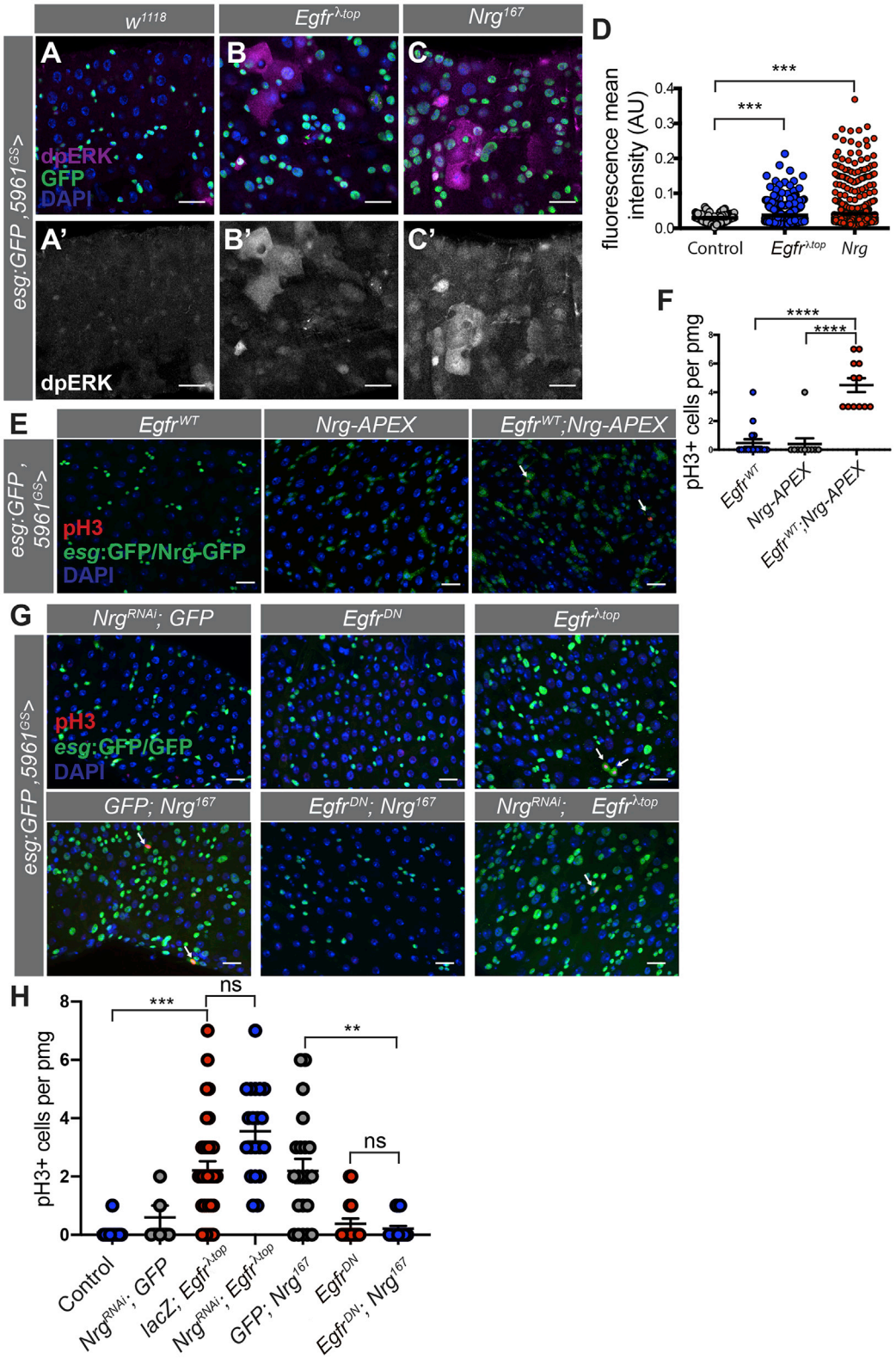

(legend on next page)

suppress age-related increases in ISC proliferation. As expected, the number of pH3^{+} cells in midguts from 28-do flies increased, compared with midguts from 7-do controls (Figures 4D, 4D′, and 4F). Depletion of *Nrg* expression in ISCs and EBs by *5961^{GS}* for 28 days blocked the age-associated increase in proliferation (Figures 4E, 4E′, and 4F). Importantly, there was no reduction in total *esg*:GFP^{+} cells over time when *Nrg^{RNAi}* was expressed, consistent with our clonal analysis data indicating Nrg is not required for ISC maintenance and that the lack of an increase in ISC proliferation is not due to loss of ISCs or EBs (Figures 1A, 1B, and 4G). These data demonstrate that depletion of Nrg from ISCs and EBs is sufficient to suppress age-related increases in ISC proliferation and the accumulation of EB-like cells.

Given that Nrg overexpression in EBs was sufficient to drive ISC proliferation, we hypothesized that endogenous Nrg expression in the EB-like cells that accumulate with age would be important in driving age-related phenotypes in the gut. Therefore, we depleted Nrg in EBs for 20 days using *Su(H)^{ts}*. Indeed, depletion of Nrg led to a significant suppression of the age-related increase in ISC proliferation compared with outcrossed controls (Figures S4A and S4B). Interestingly, depletion of Nrg in the midgut using the *5966^{GS}* Gene-Switch driver also suppressed the increase in ISC proliferation associated with age (Figures S4C and S4D). We hypothesize that this is due to the expression of *5966^{GS}*, which is expressed primarily in ECs in young flies and in both EB-like cells and ECs in intestines from aged flies (Figures S4E and S4F). Taken together, these data suggest that expression of Nrg in EBs in young flies and in EB-like cells in the guts of aged flies plays an important role in altered ISC behavior and loss of intestinal homeostasis over time.

Nrg induces ISC proliferation through the EGFR pathway

As noted above, although Nrg is commonly thought to act at the SJ, its role in ISCs and EBs is not likely to be in mediating intestinal barrier function and paracellular flux. Interestingly, previous studies showed that Nrg and hL1CAM can activate signaling via receptor tyrosine kinases (RTKs) such as EGFR and FGFR (Donier et al., 2012; García-Alonso et al., 2000; Islam et al., 2004; Kulahin et al., 2008; Nagaraj et al., 2009). Indeed, genetic analyses have shown that Egfr acts downstream of Nrg in the *Drosophila* brain and that the Nrg-Egfr pathway acts to control growth cone decisions during sensory axon guidance and axonal pathfinding during wing development (García-Alonso et al., 2000; Islam et al., 2004). Furthermore, it has been shown that in S2 cells, Egfr and Nrg interact physically, in *trans* and *cis* configurations, which result in Nrg-mediated activation of Egfr in the absence of classic Egfr ligands (Islam et al., 2004). The interaction between Nrg and Egfr is notable due to the role that the EGFR signaling pathway plays in regulating ISC proliferation and maintenance in the adult fly midgut. Egfr is essential for ISC proliferation under homeostatic conditions, as well as in response to stress signals (Biteau and Jasper, 2011; Buchon et al., 2010; Jiang and Edgar, 2009; Jiang et al., 2011; Jin et al., 2015; Wang et al., 2014a; Xu et al., 2011). Importantly, phenotypes caused by *Nrg/L1CAM* overexpression in ISCs and EBs (Figure 3A) are similar to the phenotypes reported for activation of Egfr in ISCs: increased proliferation and accumulation of EB-like cells (Biteau and Jasper, 2011; Xu et al., 2011) (Figure 3B).

To determine whether Nrg activates Egfr signaling in ISCs and EBs, we monitored the activity of the Egfr signaling pathway by detecting the levels of the active diphosphorylated form of ERK (dpERK) (Biteau and Jasper, 2011; Gabay et al., 1997; Xu et al., 2011) (Figures 5A–5D). We quantified dpERK intensity in *esg*-positive (GFP^{+}) cells in guts of flies overexpressing *Nrg* in ISCs and EBs for 7 days and compared the levels of activation with expression of a *w^{1118}* outcross (Figures 5A–5D). Expression of an activated form of Egfr, *Egfr$^{\lambda top}$*, which signals independent of any

Figure 5. Nrg interacts with Egfr to potentiate signaling

(A–C) Images of the target of Egfr signaling, dpERK (magenta/gray), in midguts expressing *w^{1118}* (A, A′), *UAS-Egfr$^{\lambda top}$* (B, B′), and *UAS-Nrg^{167}* (C, C′) driven by *5961^{GS}* for 7 days. Scale bars, 20μm.

(D) Quantification of nuclear dpERK intensity in GFP^{+} DAPI^{+} cells in (A–C). n = 108 *w^{1118}* cells, 868 *Egfr$^{\lambda top}$* cells, and 561 *Nrg^{167}* cells. Ordinary one-way ANOVA with Tukey's multiple comparisons. ***p <0.001.

(E) Representative images from adult midguts of *UAS-Egfr^{WT}*, *UAS-Nrg^{167}-APEX-GFP*, and *UAS-Egfr^{WT}; UAS-Nrg^{167}-APEX-GFP* together driven by *5961^{GS}* for 7 days. ISCs/EBs (*esg:GFP*, green), mitotic cells (pH3, red), and nuclei (DAPI, blue) are shown. White arrows indicate pH3+ cells. Scale bars, 20μm.

(F) Quantification of the number of pH3^{+} mitotic cells per pmg in (E). n = 17 *Egfr^{WT}*, 10 *Nrg^{167}-APEX-GFP*, and 12 *Egfr^{WT}; Nrg^{167}-APEX-GFP* midguts. Kruskal-Wallis test with Dunn's multiple comparisons. ****p < 0.0001.

(G) Representative images from adult midguts from epistasis analysis of *Nrg* and *Egfr* driven by *5961^{GS}* for 7 days. ISCs/EBs (*esg:GFP*, green), mitotic cells (pH3, red), and nuclei (DAPI, blue) are shown. White arrows indicate pH3+ cells. Scale bars, 20μm.

(H) Quantification of number pH3^{+} mitotic cells per pmg in (G). n = 13 control, 5 *Nrg^{RNAi}; GFP*, 33 *lacZ; Egfr$^{\lambda top}$*, 20 *Nrg^{RNAi}; Egfr$^{\lambda top}$*, 21 *GFP; Nrg^{167}*, 16 *Egfr^{DN}*, and 19 *Egfr^{DN}; Nrg^{167}* midguts, Kruskal-Wallis test followed by Dunn's multiple comparisons. ns = not significant. **p < 0.01, ***p <0.001.

All data are represented as the mean ± SEM. See also Figure S4.

ligands (Figures 5B, 5B′, and 5D), provided a positive control for dpERK staining. Our analysis showed a similar increase in dpERK intensity when comparing ectopic expression of *Nrg* and $Egfr^{\lambda top}$ with controls (Figures 5A–5D).

Unlike $Egfr^{\lambda top}$, wild-type Egfr acts in a ligand-dependent manner (Guichard et al., 1999). To test whether Nrg could enhance activation of wild-type Egfr, we co-expressed a GFP-tagged form of Nrg (*Nrg-APEX-GFP*) and wild-type Egfr ($Egfr^{WT}$) with 5961^{GS} to express in ISCs and EBs. No increase in pH3 was observed as a consequence of $Egfr^{WT}$ expression or expression of *Nrg-APEX-GFP* (Figures 5E and 5F). However, co-expression of *Nrg-APEX-GFP* together with $Egfr^{WT}$ led to a significant increase in ISC proliferation after 7 days of induction (Figures 5E and 5F), indicating that Nrg can potentiate Egfr activation to drive ISC proliferation.

Next, we wanted to determine whether Nrg acts up- or downstream of Egfr to stimulate ISC proliferation. As previously observed, overexpression of Nrg^{167} or activated $Egfr^{\lambda top}$ was sufficient to induce ISC proliferation (Figures 3C, 3D, 5G, and 5H) (Biteau and Jasper, 2011; Buchon et al., 2010; Jiang et al., 2011; Wang et al., 2014a; Xu et al., 2011). Also as expected, suppression of Egfr signaling in ISCs and EBs for 7 days, achieved by ectopic expression of a dominant-negative version of Egfr, $Egfr^{DN}$, had no observable effect on ISC or EB proliferation in intestines from young flies due to predictably low levels of proliferation (Figures 5G and 5H) (Biteau and Jasper, 2011; Xu et al., 2011). However, expression of $Egfr^{DN}$ was sufficient to suppress the increase in ISC proliferation in response to ISC/EB-specific overexpression of Nrg^{167} (Figures 4G and 4H). In contrast, RNAi-mediated depletion of *Nrg* did not suppress the increase in ISC division caused by $Egfr^{\lambda top}$. Altogether, these data indicate that Egfr signaling is activated downstream of Nrg. In addition, our data suggest that Nrg potentiation of Egfr signaling is important for the proper regulation of ISC behavior in young flies. Thus, we conclude that the increase in Nrg-expressing EB-like cells in intestines of aged flies likely contributes to an increase in ISC proliferation by enhancing Egfr activation, which contributes to the loss of gut homeostasis over time.

DISCUSSION

Nrg has been characterized previously for its signaling and cell adhesion roles in neural development (Enneking et al., 2013; Goossens et al., 2011; Kristiansen et al., 2005; Kudumala et al., 2013; Moscoso and Sanes, 1995). Additional work, including studies from our lab, has described expression and roles for Nrg in SJs in the hindgut and other epithelial tissues (Baumann, 2001; Bergstralh et al., 2015; Genova and Fehon, 2003; Resnik-Docampo et al., 2017; Wei et al., 2004). Here, we show that Nrg is a marker of ISCs and EBs in *Drosophila* and that Nrg plays a role in maintaining intestinal homeostasis. Although other SJ proteins that are expressed in ECs have been shown to regulate ISC behavior in a non-autonomous manner (Chen et al., 2020; Resnik-Docampo et al., 2017; Salazar et al., 2018; Xu et al., 2019), the restriction of Nrg expression to ISC/EB nests (Figures 1 and S1) (Baumann, 2001; Hung et al., 2020), together with the absence of SJs between ISCs and EBs, indicated another role for Nrg in the *Drosophila* midgut.

Using clonal analysis and RNAi-mediated depletion, we have identified Nrg as a novel regulator of ISC proliferation (Figures 2 and S2). Furthermore, ectopic expression of either Nrg or its human homolog, hL1CAM, was sufficient to induce proliferation and accumulation of cells expressing the ISC/EB marker, *esg* (Figure 3). Interestingly, ectopic expression in EBs alone was sufficient to cause ISC proliferation, while expression in ISCs alone was not (Figure 3), indicating Nrg can act in a non-autonomous manner to stimulate ISC proliferation.

Consistent with expression in EBs and the expansion of EB-like cells with age, an increase in cells expressing Nrg was observed in intestines from aged flies (Figures 4 and S4). Supporting the idea that the increase in Nrg-expressing cells can drive age-related ISC proliferation, depletion of Nrg from EB-like cells was also sufficient to suppress an increase in ISC proliferation in aged flies (Figures 4 and S4).

In both neurons and epithelial cells in flies, Nrg has been shown to genetically and physically interact with and potentiate the signaling of RTKs such as the EGFR and FGFR (García-Alonso et al., 2000; Islam et al., 2004). In addition, hL1CAM has been shown to bind to the EGFR to potentiate EGFR/ERK signaling *in vitro* (Donier et al., 2012; Enneking et al., 2013; Nagaraj et al., 2009). Numerous studies have indicated that EGFR signaling is an essential regulator of ISC proliferation (Biteau and Jasper, 2011; Buchon et al., 2010; Jiang et al., 2011; Jin et al., 2015; Xu et al., 2011; Zhang et al., 2019); therefore, we tested whether Nrg was important for Egfr signaling in the intestine. Consistent with its role in other tissues, we found that Nrg in ISCs and EBs of the *Drosophila* midgut acts together with Egfr to regulate mitogenic signaling (Figure 5). Therefore, our data support a model in which increases in EB-like cells with age would lead to increased Nrg, which in turn enhances Egfr signaling, resulting in uncontrolled ISC divisions and, ultimately, intestinal dysplasia.

Previous research has shown that Nrg/hL1CAM can signal through both heterotypic and homotypic binding at cell-cell contacts to potentiate signaling (Donier et al., 2012; Enneking et al., 2013; Islam et al., 2004). Further, Nrg was capable of activating Egfr/ERK signaling in the absence of additional ligands *in vitro* (Islam et al., 2004). In the *Drosophila* midgut, the Egfr ligands Vein (secreted

by visceral muscle) and Keren and Spitz (from progenitors and ECs) have been described to stimulate ISC proliferation primarily during homeostasis and stress (Biteau and Jasper, 2011; Buchon et al., 2010; Jiang et al., 2011; Patel et al., 2015; Xu et al., 2011). Limited data are available on the participation of the various ligands in Egfr activation with aging. Therefore, further research is needed to determine whether Nrg may activate Egfr independently or in conjunction with traditional agonists.

It is important to note that Nrg may activate Egfr signaling in the fly midgut using mechanisms other than direct physical interaction. For example, loss of other SJ proteins in ECs or adhesion proteins, such E-cadherin, in ISCs and EBs can lead to Egfr/ERK activation, indirectly, via stress-mediated increases in transcription and post-translational processing of Egfr ligands or of Egfr itself (Chen et al., 2020; Ngo et al., 2020; Resnik-Docampo et al., 2017; Salazar et al., 2018; Xu et al., 2019). Additional studies will be needed to uncover the mechanism(s) by which Nrg regulates Egfr signaling and activation in ISCs and EBs of the fly intestine.

Intriguingly, recent research has identified age-related disruption of the endocytosis/autophagy pathway as one mechanism leading to an increase in Egfr and, consequently, ERK signaling in ISCs via stabilization of the ligand-activated Egfr (Du et al., 2020; Zhang et al., 2019). Our work suggests that an increase in Nrg-mediated potentiation of Egfr signaling is an additional mechanism that contributes to increases in ISC proliferation and intestinal dysplasia with age (Figures 4 and S4).

Increased hL1CAM expression is associated with a variety of cancers (Altevogt et al., 2016; Gavert et al., 2008) and tumor metastasis (Ernst et al., 2018; Fang et al., 2020; Gavert et al., 2010; Huszar et al., 2010; Lund et al., 2015; Terraneo et al., 2020), including gastrointestinal cancers (Fang et al., 2020; Ganesh et al., 2020; Gavert et al., 2005, 2010). Mechanistic studies have shown that increases in hL1CAM may be associated with the endothelial to mesenchymal transition to drive metastasis (Ernst et al., 2018; Giordano and Cavallaro, 2020; Huszar et al., 2010; Lund et al., 2015; Tischler et al., 2011; Versluis et al., 2018). In addition, hL1CAM was required for growth and proliferation of intestinal organoids derived from colorectal cancer (CRC) tissue (Ganesh et al., 2020). Indeed, increases in hL1CAM have been shown to regulate CRC metastasis via ERK signaling (Fang et al., 2020), indicating that the relationship between Nrg and Egfr may be conserved in the mammalian intestine. Therefore, a better understanding of the role of Nrg/hL1CAM-EGFR signaling in stem cell proliferation and maintenance may lead to the development of new strategies to target this pathway in the initiation and progression of CRC and disorders caused by excess EGFR activation.

EXPERIMENTAL PROCEDURES

Fly food and husbandry

All analyses for these studies were performed on female flies, as age-related gut pathology has been well established in females (Biteau et al., 2008; Rera et al., 2012).

Flies were cultured in vials containing standard cornmeal medium (1% agar, 3% brewer's yeast, 1.9% sucrose, 7.7% molasses or 7.8% malt syrup, and 9.1% cornmeal; all concentrations given in wt/vol). For experiments using the drug-inducible GAL4 Gene-Switch (Osterwalder et al., 2001; Roman et al., 2001) driver, flies were crossed to UAS-Nrg^{RNAi} or UAS-Nrg^{167} or outcrossed to control (UAS-$mCherry^{RNAi}$ or w^{1118}) and raised at 25°C. Progeny were allowed to mate and develop for 3–5 days before being transferred to food mixed with 50 μg/mL mifepristone (RU486, Sigma) or ethanol

STOCK	SOURCE	IDENTIFIER
Su(H)lacZ; esg:GFP,5961-GAL4^{GS}	gift from B. Ohlstein, Columbia University, USA (Mathur et al., 2010)	
Su(H)lacZ; esg:GFP,5966-GAL4^{GS}	gift from B. Ohlstein, Columbia University, USA	
Su(H)-GAL4, UAS-CD8GFP; tubGAL80^{ts}	gift from S. Hou (Zeng et al., 2010)	
esg-GAL4, UAS-2xYFP; Su(H)GAL80, tubGAL80^{ts}	gift from S. Hou (Wang et al., 2014b)	
SalEPGAL4	gift from J.F. de Celis	
y,w,hsFLP1.22 P[tub-gal4] UAS-GFP; P[tub-gal80^{ts}] FRT40A/CyO	gift from A. Baonza, CBMSO, Spain	
Nrg^{HMS01638} Valium 20		BDSC 37496
Nrg^{GD14467}		VDRC 27201
Nrg^{14} FRT19A	gift from Jan Pielage, Division of Zoology-Neurobiology, Technische Universität Kaiserslautern, Germany	
Nrg^{G00413} FRT19A		Kyoto stock center 111923
UAS-Nrg^{167}		BDSC 24172
UAS-hL1CAM	Islam et al. (2004	BDSC 24171
UAS-Egfr$^{\lambda top}$		BDSC 59843
UAS-Egfr^{DN}		BDSC 5364
UAS-Egfr^{WT}		BDSC 5368
Neuroglian::GFP (Nrg::GFP)	gift from G. Tanentzapf, University of British Columbia, Canada	

(control) at 25°C. Flies were transferred to new food vials every 2–3 days. Aged flies in Figures 4D and 4E were induced for the entire aging interval. For temperature-sensitive (ts) crosses using GAL80^{ts}, crosses were set and maintained at 18°C until eclosion. Adults were kept for 2–3 days at 18°C and then moved to 29°C for the time noted.

Fly lines

Lines not described in the text can be found in Flybase.

Generation of Neuroglian antibody

The Nrg antibody was designed and generated by Thermo Fisher Scientific. A synthetic peptide from the C-terminal *Nrg* sequence 1204:1222:KPGVESDTDSMAEYGDGDT was generated and used to inject rabbits. Antisera were collected after 96 days. Unpurified sera were used for IF.

Fluorescence microscopy and antibody staining

Imaging was always done on the P3–P4 regions of the *Drosophila* intestine, located by centering the pyloric ring in a ×40 field of view (fov) and moving 1–2 fov toward the anterior. Midguts were dissected into ice-cold phosphate-buffered saline (PBS)/4% paraformaldehyde (PFA) and incubated for 1 h in fixative at room temperature, followed by three 10-min washes in PBT (PBS containing 0.1% Triton X-100), and incubated in blocking solution (PBT-0.5% or PBT-0.3% bovine serum albumin) for 30 min. Samples were placed in primary antibody overnight at 4°C, washed 4 × 5 min at room temperature in PBT, incubated with secondary antibodies at room temperature for 2 h, washed three times with PBT, and mounted in Vectashield with DAPI (Vector Laboratories, H-1200).

For anti-dpERK staining, the following protocol was modified from Castanieto et al. (2014). Flies were placed on food supplemented with yeast paste overnight prior to dissection. Posterior midguts were dissected into ice-cold PBS with phosphatase inhibitor (1:100, Sigma, cat. no. P5726). Guts were fixed in ice-cold PBS/4% PFA with phosphatase inhibitor and then taken through a methanol (MeOH) dehydration as follows: 25% MeOH 3 min, 50% MeOH 3 min, 75% MeOH 3 min, 100% MeOH 3 min, 75% MeOH 3 min, 50% MeOH 3 min, 25% MeOH 3 min. All MeOH solutions contained phosphatase inhibitors. Guts were washed three times, for 10 min each, in PBT plus phosphatase inhibitor and then were immunostained, as above, with the addition of phosphatase inhibitor in all solutions.

Primary antibodies used included rabbit anti-GFP (1:3,000, Molecular Probes A-11122), mouse anti-GFP (1:200, Molecular Probes A-11120), chicken anti-GFP (1:500, Aves Labs GFP-1010), rabbit anti-β-gal (1:2,000, Cappel/MPbio 559761), mouse anti-β-gal (1:20, DSHB 40-1a), rabbit anti-pH3 (1:200, Millipore 06-570), rabbit anti-dsRed (1:100, Clontech, 632496), rabbit anti-Nrg (1:50, this study), mouse anti-Egfr (1:1,000, Millipore Sigma E2906), and rabbit anti-phospho-p44/42 MAPK (1:100 Cell Signaling Technology, cat. no. 4370). The Armadillo antibody used (mouse, 1:100) was obtained from the Developmental Studies Hybridoma Bank, developed under the auspices of the NICHD and maintained by The University of Iowa, Department of Biology, Iowa City, Iowa 52242.

Images were acquired on a Zeiss LSM710 or LSM800 inverted confocal microscope, and/or on a Zeiss Axio Observer Z1, and processed with Fiji/ImageJ (NIH) and Zen Blue or Black software (Zeiss). The final figures were assembled using Adobe Photoshop or Adobe Illustrator.

Generation of MARCM clones

For mutant clones, *hs-flp,tubGal80, neoFRT19A; UAS-mCD8::GFP* flies were crossed to *FRT19A, Nrg^{14}/FM7; P[tub-Gal4]/CyO* or *FRT19A, Nrg^{G00413}/FM7; P[tub-Gal4]/CyO* or *FRT19A/FM7; P[tub-Gal4]/CyO* (control) flies (Figure 2).

For RNAi clones, *y,w,hsFLP1.22 P[tub-Gal4] UAS-GFP; P[tub-Gal80^{ts}] FRT40A/CyO* flies were crossed to *FRT40A/CyO; UAS-Nrg$^{RNAi\ GD}$/TM6B* or *FRT40A/CyO; 2xUAS-GFP/TM6B* (control) (Figure S2).

Progeny raised at 25°C were heat shocked at 37°C for 90 min once or twice on the same day, 6–7 h apart. The flies were placed back at 25°C and dissected at designated time points, as noted in figure legends.

Generation of *UAS-Nrg-APEX2-GFP*

APEX2-EGFP (a gift from M. Ellisman) was inserted into the vector pUASt attBK7 SfiI BglII EcoRI (a gift from M. Rera and D. Walker, UCLA). Full-length Nrg cDNA obtained from DGRC (clone GH03573) was inserted into the linearized backbone (EcoRI, SfiI) using an In-Fusion HD Cloning Kit (Takara Bio). Site-specific attp40 insertion into the fly genome was performed by Bestgene, Inc.

Statistics and reproducibility

Statistical analysis and graphical display of the data were performed using Prism9 (GraphPad). Significance, expressed as p values, was determined with a two-tailed test; all tests used were as indicated in the figure legends: one-way ANOVA/Tukey's multiple comparisons test or Student's t test was used when data met the criteria for parametric analysis (normal distribution, equal variances), and Kruskal-Wallis/Dunn multiple comparisons test was used when data were non-parametric. Experiments were repeated at least two times. No statistical method was used to predetermine sample size. The experiments were not randomized and investigators were not blinded to allocation during experiments and outcome assessment.

Data and code availability

RNA-sequencing data were previously published (Resnik-Docampo et al., 2017) and deposited in the Gene Expression Omnibus under the accession no. GSE74171. All other data supporting the findings of this study are available from the corresponding author on request.

SUPPLEMENTAL INFORMATION

Supplemental information can be found online at https://doi.org/10.1016/j.stemcr.2021.04.006.

AUTHOR CONTRIBUTIONS

M.R.-D., K.M.C., and D.L.J. designed experiments. M.R.-D., K.M.C., S.M.R., C.C., and V.S. designed and tested reagents, performed experiments, and analyzed the data. K.M.C., M.R.-D., and D.L.J. wrote and edited the manuscript.

ACKNOWLEDGMENTS

The authors thank H. Jasper (Genentech and The Buck Institute for Research on Aging, USA), Ben Ohlstein (Columbia University, USA), J. Pielage (University of Kaiserslautern, Germany), J.F. de Celis (CBMSO, Spain), A. Baonza (CBMSO, Spain), G. Tanentzapf (University of British Columbia, Canada), the Vienna Drosophila RNAi Center (VDRC), Kyoto Stock Center (DGRC), and Bloomington Stock Center for reagents; the BSCRC/MCDB microscopy core at UCLA; and the Jones laboratory for comments on the manuscript.

This work was supported by the Eli & Edythe Broad Center of Regenerative Medicine & Stem Cell Research (D.L.J.), the UCLA Tumor Cell Biology Training Program (USHHS Ruth L. Kirschstein Institutional National Research Service Award T32 CA009056) (K.M.C.), a National Rosacea Society Award F32GM119394 (C.C.), the Center for Opportunities to Maximize Participation, Access, and Student Success in the Life Sciences (COMPASS Life Sciences) (S.M.R.), and the NIH NIGMS Individual Postdoctoral Ruth L. Kirschstein National Research Service Award R01AG028092, R01DK105442, and R01GM135767 (D.L.J.).

Received: September 20, 2020
Revised: April 11, 2021
Accepted: April 12, 2021
Published: May 6, 2021

SUPPORTING CITATIONS

The following references appear in the supplemental information: Berg et al., 2019; Carpenter et al., 2006; Kamentsky et al., 2011.

REFERENCES

Altevogt, P., Doberstein, K., and Fogel, M. (2016). L1CAM in human cancer. Int. J. Cancer *138*, 1565–1576.

Amcheslavsky, A., Song, W., Li, Q., Nie, Y., Bragatto, I., Ferrandon, D., Perrimon, N., and Ip, Y.T. (2014). Enteroendocrine cells support intestinal stem-cell-mediated homeostasis in Drosophila. Cell Rep. *9*, 32–39.

Baumann, O. (2001). Posterior midgut epithelial cells differ in their organization of the membrane skeleton from other drosophila epithelia. Exp. Cell Res. *270*, 176–187.

Berg, S., Kutra, D., Kroeger, T., Straehle, C.N., Kausler, B.X., Haubold, C., Schiegg, M., Ales, J., Beier, T., Rudy, M., et al. (2019). ilastik: interactive machine learning for (bio)image analysis. Nat. Methods *16*, 1226–1232.

Bergstralh, D.T., Lovegrove, H.E., and St Johnston, D. (2015). Lateral adhesion drives reintegration of misplaced cells into epithelial monolayers. Nat. Cell Biol. *17*, 1497–1503.

Biteau, B., and Jasper, H. (2011). EGF signaling regulates the proliferation of intestinal stem cells in Drosophila. Development *138*, 1045–1055.

Biteau, B., and Jasper, H. (2014). Slit/Robo signaling regulates cell fate decisions in the intestinal stem cell lineage of Drosophila. Cell Rep. *7*, 1867–1875.

Biteau, B., Hochmuth, C.E., and Jasper, H. (2008). JNK activity in somatic stem cells causes loss of tissue homeostasis in the aging Drosophila gut. Cell Stem Cell *3*, 442–455.

Buchon, N., Broderick, N.A., Kuraishi, T., and Lemaitre, B. (2010). Drosophila EGFR pathway coordinates stem cell proliferation and gut remodeling following infection. BMC Biol. *8*, 152.

Carpenter, A.E., Jones, T.R., Lamprecht, M.R., Clarke, C., Kang, I.H., Friman, O., Guertin, D.A., Chang, J.H., Lindquist, R.A., Moffat, J., et al. (2006). CellProfiler: image analysis software for identifying and quantifying cell phenotypes. Genome Biol. *7*, R100.

Castanieto, A., Johnston, M.J., and Nystul, T.G. (2014). EGFR signaling promotes self-renewal through the establishment of cell polarity in Drosophila follicle stem cells. Elife *3*, e04437.

Chen, H.-J., Li, Q., Nirala, N.K., and Ip, Y.T. (2020). The Snakeskin-Mesh complex of smooth septate junction Restricts Yorkie to regulate intestinal homeostasis in Drosophila. Stem Cell Reports *14*, 828–844.

Cordero, J.B., Stefanatos, R.K., Myant, K., Vidal, M., and Sansom, O.J. (2012). Non-autonomous crosstalk between the Jak/Stat and Egfr pathways mediates Apc1-driven intestinal stem cell hyperplasia in the Drosophila adult midgut. Development *139*, 4524–4535.

Dahme, M., Bartsch, U., Martini, R., Anliker, B., Schachner, M., and Mantei, N. (1997). Disruption of the mouse L1 gene leads to malformations of the nervous system. Nat. Genet. *17*, 346–349.

Donier, E., Gomez-Sanchez, J.A., Grijota-Martinez, C., Lakomá, J., Baars, S., Garcia-Alonso, L., and Cabedo, H. (2012). L1CAM binds ErbB receptors through Ig-like domains coupling cell adhesion and neuregulin signalling. PLoS One *7*, e40674.

Du, G., Qiao, Y., Zhuo, Z., Zhou, J., Li, X., Liu, Z., Li, Y., and Chen, H. (2020). Lipoic acid rejuvenates aged intestinal stem cells by preventing age-associated endosome reduction. EMBO Rep. *21*, e49583.

Enneking, E.-M., Kudumala, S.R., Moreno, E., Stephan, R., Boerner, J., Godenschwege, T.A., and Pielage, J. (2013). Transsynaptic coordination of synaptic growth, function, and stability by the L1-type CAM Neuroglian. Plos Biol. *11*, e1001537.

Ernst, A.-K., Putscher, A., Samatov, T.R., Suling, A., Galatenko, V.V., Shkurnikov, M.Y., Knyazev, E.N., Tonevitsky, A.G., Haalck, T., Lange, T., et al. (2018). Knockdown of L1CAM significantly reduces metastasis in a xenograft model of human melanoma: L1CAM is a potential target for anti-melanoma therapy. PLoS One *13*, e0192525.

Fang, Q.-X., Zheng, X.-C., and Zhao, H.-J. (2020). L1CAM is involved in lymph node metastasis via ERK1/2 signaling in colorectal cancer. Am. J. Transl. Res. *12*, 837–846.

Gabay, L., Seger, R., and Shilo, B.Z. (1997). In situ activation pattern of Drosophila EGF receptor pathway during development. Science *277*, 1103–1106.

Ganesh, K., Basnet, H., Kaygusuz, Y., Laughney, A.M., He, L., Sharma, R., O'Rourke, K.P., Reuter, V.P., Huang, Y.-H., Turkekul, M., et al. (2020). L1CAM defines the regenerative origin of metastasis-initiating cells in colorectal cancer. Nat. Cancer *1*, 28–45.

García-Alonso, L., Romani, S., and Jiménez, F. (2000). The EGF and FGF receptors mediate neuroglian function to control growth cone

decisions during sensory axon guidance in Drosophila. Neuron *28*, 741–752.

Gavert, N., Conacci-Sorrell, M., Gast, D., Schneider, A., Altevogt, P., Brabletz, T., and Ben-Ze'ev, A. (2005). L1, a novel target of beta-catenin signaling, transforms cells and is expressed at the invasive front of colon cancers. J. Cell Biol. *168*, 633–642.

Gavert, N., Ben-Shmuel, A., Raveh, S., and Ben-Ze'ev, A. (2008). L1-CAM in cancerous tissues. Expert Opin. Biol. Ther. *8*, 1749–1757.

Gavert, N., Ben-Shmuel, A., Lemmon, V., Brabletz, T., and Ben-Ze'ev, A. (2010). Nuclear factor-kappaB signaling and ezrin are essential for L1-mediated metastasis of colon cancer cells. J. Cell Sci. *123*, 2135–2143.

Genova, J.L., and Fehon, R.G. (2003). Neuroglian, Gliotactin, and the Na+/K+ ATPase are essential for septate junction function in Drosophila. J. Cell Biol. *161*, 979–989.

Giordano, M., and Cavallaro, U. (2020). Different shades of L1CAM in the pathophysiology of cancer stem cells. J. Clin. Med. *9*, 1502.

Godenschwege, T.A., Kristiansen, L.V., Uthaman, S.B., Hortsch, M., and Murphey, R.K. (2006). A conserved role for Drosophila Neuroglian and human L1-CAM in central-synapse formation. Curr. Biol. *16*, 12–23.

Goossens, T., Kang, Y.Y., Wuytens, G., Zimmermann, P., Callaerts-Végh, Z., Pollarolo, G., Islam, R., Hortsch, M., and Callaerts, P. (2011). The Drosophila L1CAM homolog Neuroglian signals through distinct pathways to control different aspects of mushroom body axon development. Development *138*, 1595–1605.

Guichard, A., Biehs, B., Sturtevant, M.A., Wickline, L., Chacko, J., Howard, K., and Bier, E. (1999). Rhomboid and Star interact synergistically to promote EGFR/MAPK signaling during Drosophila wing vein development. Development *126*, 2663–2676.

Guo, Z., and Ohlstein, B. (2015). Stem cell regulation. Bidirectional Notch signaling regulates Drosophila intestinal stem cell multipotency. Science *350*, aab0988.

Hortsch, M., Bieber, A.J., Patel, N.H., and Goodman, C.S. (1990). Differential splicing generates a nervous system-specific form of Drosophila neuroglian. Neuron *4*, 697–709.

Hung, R.-J., Hu, Y., Kirchner, R., Liu, Y., Xu, C., Comjean, A., Tattikota, S.G., Li, F., Song, W., Ho Sui, S., et al. (2020). A cell atlas of the adult Drosophila midgut. Proc. Natl. Acad. Sci. U S A *117*, 1514–1523.

Huszar, M., Pfeifer, M., Schirmer, U., Kiefel, H., Konecny, G.E., Ben-Arie, A., Edler, L., Münch, M., Müller-Holzner, E., Jerabek-Klestil, S., et al. (2010). Up-regulation of L1CAM is linked to loss of hormone receptors and E-cadherin in aggressive subtypes of endometrial carcinomas. J. Pathol. *220*, 551–561.

Islam, R., Wei, S.-Y., Chiu, W.-H., Hortsch, M., and Hsu, J.-C. (2003). Neuroglian activates Echinoid to antagonize the Drosophila EGF receptor signaling pathway. Development *130*, 2051–2059.

Islam, R., Kristiansen, L.V., Romani, S., Garcia-Alonso, L., and Hortsch, M. (2004). Activation of EGF receptor kinase by L1-mediated homophilic cell interactions. Mol. Biol. Cell *15*, 2003–2012.

Jasper, H. (2020). Intestinal stem cell aging: origins and interventions. Annu. Rev. Physiol. *82*, 203–226.

Jiang, H., and Edgar, B.A. (2009). EGFR signaling regulates the proliferation of Drosophila adult midgut progenitors. Development *136*, 483–493.

Jiang, H., Patel, P.H., Kohlmaier, A., Grenley, M.O., McEwen, D.G., and Edgar, B.A. (2009). Cytokine/Jak/Stat signaling mediates regeneration and homeostasis in the Drosophila midgut. Cell *137*, 1343–1355.

Jiang, H., Grenley, M.O., Bravo, M.-J., Blumhagen, R.Z., and Edgar, B.A. (2011). EGFR/Ras/MAPK signaling mediates adult midgut epithelial homeostasis and regeneration in Drosophila. Cell Stem Cell *8*, 84–95.

Jin, Y., Ha, N., Forés, M., Xiang, J., Gläßer, C., Maldera, J., Jiménez, G., and Edgar, B.A. (2015). EGFR/Ras signaling controls Drosophila intestinal stem cell proliferation via capicua-regulated genes. PLoS Genet. *11*, e1005634.

Jones, D.L., and Rando, T.A. (2011). Emerging models and paradigms for stem cell ageing. Nat. Cell Biol. *13*, 506–512.

Jouet, M., Rosenthal, A., Armstrong, G., MacFarlane, J., Stevenson, R., Paterson, J., Metzenberg, A., Ionasescu, V., Temple, K., and Kenwrick, S. (1994). X-linked spastic paraplegia (SPG1), MASA syndrome and X-linked hydrocephalus result from mutations in the L1 gene. Nat. Genet. *7*, 402–407.

Kakad, P.P., Penserga, T., Davis, B.P., Henry, B., Boerner, J., Riso, A., Pielage, J., and Godenschwege, T.A. (2018). An ankyrin-binding motif regulates nuclear levels of L1-type neuroglian and expression of the oncogene Myc in Drosophila neurons. J. Biol. Chem. *293*, 17442–17453.

Kamentsky, L., Jones, T.R., Fraser, A., Bray, M.-A., Logan, D.J., Madden, K.L., Ljosa, V., Rueden, C., Eliceiri, K.W., and Carpenter, A.E. (2011). Improved structure, function and compatibility for CellProfiler: modular high-throughput image analysis software. Bioinformatics *27*, 1179–1180.

Kristiansen, L.V., Velasquez, E., Romani, S., Baars, S., Berezin, V., Bock, E., Hortsch, M., and Garcia-Alonso, L. (2005). Genetic analysis of an overlapping functional requirement for L1- and NCAM-type proteins during sensory axon guidance in Drosophila. Mol. Cell. Neurosci. *28*, 141–152.

Kudumala, S., Freund, J., Hortsch, M., and Godenschwege, T.A. (2013). Differential effects of human L1CAM mutations on complementing guidance and synaptic defects in Drosophila melanogaster. PLoS One *8*, e76974.

Kulahin, N., Li, S., Hinsby, A., Kiselyov, V., Berezin, V., and Bock, E. (2008). Fibronectin type III (FN3) modules of the neuronal cell adhesion molecule L1 interact directly with the fibroblast growth factor (FGF) receptor. Mol. Cell. Neurosci. *37*, 528–536.

Li, H., and Jasper, H. (2016). Gastrointestinal stem cells in health and disease: from flies to humans. Dis. Model. Mech. *9*, 487–499.

Lund, K., Dembinski, J.L., Solberg, N., Urbanucci, A., Mills, I.G., and Krauss, S. (2015). Slug-dependent upregulation of L1CAM is responsible for the increased invasion potential of pancreatic cancer cells following long-term 5-FU treatment. PLoS One *10*, e0123684.

Marchiando, A.M., Graham, W.V., and Turner, J.R. (2010). Epithelial barriers in homeostasis and disease. Annu. Rev. Pathol. *5*, 119–144.

Mathur, D., Bost, A., Driver, I., and Ohlstein, B. (2010). A transient niche regulates the specification of Drosophila intestinal stem cells. Science *327*, 210–213.

Micchelli, C.A., and Perrimon, N. (2006). Evidence that stem cells reside in the adult Drosophila midgut epithelium. Nature *439*, 475–479.

Moscoso, L.M., and Sanes, J.R. (1995). Expression of four immunoglobulin superfamily adhesion molecules (L1, Nr-CAM/Bravo, neurofascin/ABGP, and N-CAM) in the developing mouse spinal cord. J. Comp. Neurol. *352*, 321–334.

Nagaraj, K., Kristiansen, L.V., Skrzynski, A., Castiella, C., Garcia-Alonso, L., and Hortsch, M. (2009). Pathogenic human L1-CAM mutations reduce the adhesion-dependent activation of EGFR. Hum. Mol. Genet. *18*, 3822–3831.

Nászai, M., Carroll, L.R., and Cordero, J.B. (2015). Intestinal stem cell proliferation and epithelial homeostasis in the adult Drosophila midgut. Insect Biochem. Mol. Biol. *67*, 9–14.

Ngo, S., Liang, J., Su, Y.-H., and O'Brien, L.E. (2020). Disruption of EGF feedback by intestinal tumors and neighboring cells in drosophila. Curr. Biol. *30*, 1537–1546.e3.

Ohlstein, B., and Spradling, A. (2006). The adult Drosophila posterior midgut is maintained by pluripotent stem cells. Nature *439*, 470–474.

Osterwalder, T., Yoon, K.S., White, B.H., and Keshishian, H. (2001). A conditional tissue-specific transgene expression system using inducible GAL4. Proc. Natl. Acad. Sci. U S A *98*, 12596–12601.

Park, J.-S., Kim, Y.-S., and Yoo, M.-A. (2009). The role of p38b MAPK in age-related modulation of intestinal stem cell proliferation and differentiation in Drosophila. Aging (Albany NY) *1*, 637–651.

Patel, P.H., Dutta, D., and Edgar, B.A. (2015). Niche appropriation by Drosophila intestinal stem cell tumours. Nat. Cell Biol. *17*, 1182–1192.

Rera, M., Clark, R.I., and Walker, D.W. (2012). Intestinal barrier dysfunction links metabolic and inflammatory markers of aging to death in Drosophila. Proc. Natl. Acad. Sci. U S A *109*, 21528–21533.

Resnik-Docampo, M., Koehler, C.L., Clark, R.I., Schinaman, J.M., Sauer, V., Wong, D.M., Lewis, S., D'Alterio, C., Walker, D.W., and Jones, D.L. (2017). Tricellular junctions regulate intestinal stem cell behaviour to maintain homeostasis. Nat. Cell Biol. *19*, 52–59.

Roman, G., Endo, K., Zong, L., and Davis, R.L. (2001). P[Switch], a system for spatial and temporal control of gene expression in Drosophila melanogaster. Proc. Natl. Acad. Sci. U S A *98*, 12602–12607.

Salazar, A.M., Resnik-Docampo, M., Ulgherait, M., Clark, R.I., Shirasu-Hiza, M., Jones, D.L., and Walker, D.W. (2018). Intestinal snakeskin limits microbial dysbiosis during aging and promotes longevity. IScience *9*, 229–243.

Schäfer, M.K.E., and Altevogt, P. (2010). L1CAM malfunction in the nervous system and human carcinomas. Cell Mol. Life Sci. *67*, 2425–2437.

Terraneo, N., Jacob, F., Peitzsch, C., Dubrovska, A., Krudewig, C., Huang, Y.-L., Heinzelmann-Schwarz, V., Schibli, R., Béhé, M., and Grünberg, J. (2020). L1 cell adhesion molecule confers radioresistance to ovarian cancer and defines a new cancer stem cell population. Cancers (Basel) *12*, 217.

Tischler, V., Pfeifer, M., Hausladen, S., Schirmer, U., Bonde, A.-K., Kristiansen, G., Sos, M.L., Weder, W., Moch, H., Altevogt, P., et al. (2011). L1CAM protein expression is associated with poor prognosis in non-small cell lung cancer. Mol. Cancer *10*, 127.

Vancamelbeke, M., and Vermeire, S. (2017). The intestinal barrier: a fundamental role in health and disease. Expert Rev. Gastroenterol. Hepatol. *11*, 821–834.

Versluis, M., Plat, A., de Bruyn, M., Matias-Guiu, X., Trovic, J., Krakstad, C., Nijman, H.W., Bosse, T., de Bock, G.H., and Hollema, H. (2018). L1CAM expression in uterine carcinosarcoma is limited to the epithelial component and may be involved in epithelial-mesenchymal transition. Virchows Arch. *473*, 591–598.

Wang, C., Guo, X., and Xi, R. (2014a). EGFR and Notch signaling respectively regulate proliferative activity and multiple cell lineage differentiation of Drosophila gastric stem cells. Cell Res. *24*, 610–627.

Wang, L., Zeng, X., Ryoo, H.D., and Jasper, H. (2014b). Integration of UPRER and oxidative stress signaling in the control of intestinal stem cell proliferation. PLoS Genet. *10*, e1004568.

Wei, J., Hortsch, M., and Goode, S. (2004). Neuroglian stabilizes epithelial structure during Drosophila oogenesis. Dev. Dyn. *230*, 800–808.

Xu, C., Tang, H.-W., Hung, R.-J., Hu, Y., Ni, X., Housden, B.E., and Perrimon, N. (2019). The septate junction protein Tsp2A restricts intestinal stem cell activity via endocytic regulation of aPKC and Hippo signaling. Cell Rep. *26*, 670–688.e6.

Xu, N., Wang, S.Q., Tan, D., Gao, Y., Lin, G., and Xi, R. (2011). EGFR, Wingless and JAK/STAT signaling cooperatively maintain Drosophila intestinal stem cells. Dev. Biol. *354*, 31–43.

Zeng, X., and Hou, S.X. (2015). Enteroendocrine cells are generated from stem cells through a distinct progenitor in the adult Drosophila posterior midgut. Development *142*, 644–653.

Zeng, X., Chauhan, C., and Hou, S.X. (2010). Characterization of midgut stem cell- and enteroblast-specific Gal4 lines in drosophila. Genesis *48*, 607–611.

Zhang, P., Holowatyj, A.N., Roy, T., Pronovost, S.M., Marchetti, M., Liu, H., Ulrich, C.M., and Edgar, B.A. (2019). An SH3PX1-dependent endocytosis-autophagy network restrains intestinal stem cell proliferation by counteracting EGFR-ERK signaling. Dev. Cell *49*, 574–589.e5.